

EXPERIMENTAL AND NUMERICAL INVESTIGATION OF FLOW CONDITIONS OVER LALELI DAM SPILLWAY

Ismail Aydin¹, Mustafa Gogus¹, Mete Koken¹ & A. Burcu Altan-Sakarya¹

¹Department of Civil Engineering, Middle East Technical University, Turkey, Dumlupinar Bulvari No:1, 06800, Ankara
E-mail: burcuas@metu.edu.tr

Abstract

The Laleli dam is located on the Coruh river in North-East Turkey. The Laleli dam spillway is laid on the downstream face of the dam body. The spillway channel starts with a gate controlled ogee crest followed by a linear prismatic channel section having a slope of 1.43 and the structure is terminated with a flip-bucket type deflector. Elevation difference between the reservoir water surface and the downstream end of the flip-bucket is 110 m.

Hydraulic model of the spillway was constructed at a length scale of 1/25 based on the Froude similarity law. The entrance conditions, flow around the dividing walls, water depths and the pressure distributions all along the centerline of the spillway chute were investigated. After determining the locations of negative pressures over the spillway chute, to eliminate the risk of cavitation, an aeration facility was designed to aerate the flow from the underneath separation nappe. The location, geometric details and performance of the aeration facility were investigated.

A numerical study was also conducted using the Flow-3D commercial CFD code to simulate the flow conditions in the model scale. Pressure distribution and the cavitation number were calculated along the spillway. Overall it has been observed that there is an agreement between the experimental and numerical model results.

Introduction

The Laleli dam is the first dam at the upstream of the Coruh river. Since there is no control structure at the upstream of this river, it will be subjected to floods with huge discharges. Because of its large slope, the Laleli dam spillway has a cavitation risk and should be investigated.

Similar studies were performed in the literature by, Kokpinar and Gogus 2002, Unami et al. 1999, Dargahi 2006 and Pfister 2011. It should be noted that all the quantities in the present paper are given for the prototype scale.

Hydraulic Model

A hydraulic model of the Laleli dam spillway with a scale of 1/25 is built in Middle East Technical University (METU) Hydraulics Laboratory (Figure 1).

The Froude similarity is used in the model where the design discharge is taken as 1080 m³/s, which is the 1000 year return period flood discharge. Total width of the spillway is 38 m, and the flow is controlled with 4 radial gates. One full gate and two halved gates are built in the hydraulic model symmetrically where half of the design discharge is passed through it. Approximately 600 m part of the reservoir is designed as an approach channel. Filter material is used in front of the pipes supplying water to the reservoir in order to regulate the flow and to damp the oscillations.



Figure 1: General view of the physical model built in METU Hydraulics Laboratory.

Elevation difference between the reservoir water surface and the downstream end of the flip-bucket is 110 m. If the crest of the spillway is assumed to be the origin, in the flow direction there is a curved surface over the spillway up to a horizontal distance of $x = 13.3$ m, then there is a straight channel until $x = 75.6$ m where the flip bucket starts. Water leaving the spillway through the flip bucket is collected in a pool and then diverted into a downstream channel. Discharge passing through the system is measured with a

rectangular sharp crested weir located at the downstream end of this channel. Starting at $x = -2.8$ m, where $x = 0$ m is the crest of the spillway, along the centerline of the whole spillway length the piezometer tubes are connected to the system to measure the piezometric heads (Figure 2).



Figure 2: Spillway crest of the physical model: a) View from the reservoir, b) Side view.

Several experiments performed is presented in this paper. Initially, the original design is tested where the flow depths and the piezometric heads are recorded, and the cavitation number is calculated along the spillway. Afterwards, the same data is obtained for the suggested spillway design which contains an aerator system.

Numerical Model

3D numerical simulation of the original spillway design is made using the commercial software Flow-3D. $k-\epsilon$ turbulence model is used in the simulation where only the water phase is resolved. Firstly the three dimensional solid model of the spillway is created, secondly the structured mesh composed of two blocks is put on top of this model (Figure 3).

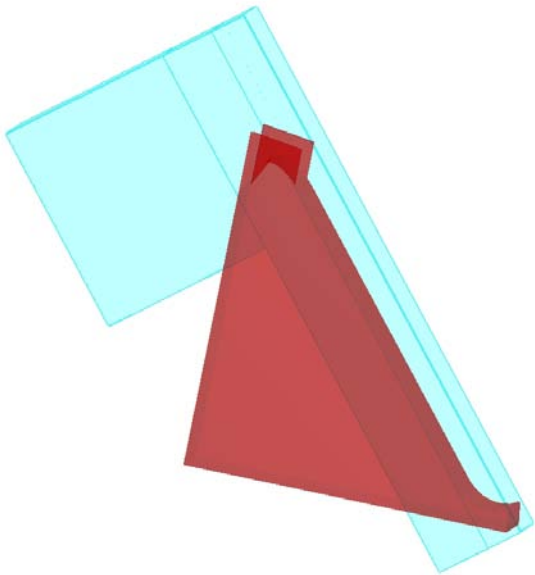


Figure 3: Spillway solid model and structured mesh blocks.

Flow-3D uses non-body fitted mesh, therefore in order to have a better control over the mesh size near the solid boundaries, the model is rotated so that it is aligned with the mesh block. Mesh points are clustered close to the spillway surface so that the first grid point was located inside the logarithmic region. Active mesh size in the simulation was around 3 million. In order to make a better comparison, model scale is used in the simulation where only one of the four openings between three piers along the spillway crest is modelled. As a result symmetry boundary condition is used at the lateral sidewalls. Water level in the reservoir is fixed so that it will pass the 1000 year return period storm discharge. Hydrostatic pressure distribution is applied on the reservoir edge. Outflow boundary condition is utilized on the other surfaces so that water can leave the domain.

Discussion of Results

Pressure heads are measured over the centerline of the spillway model using the piezometer tubes (Figure 4). Here TR-1 represents the original design whereas TR-4 is the design which contains an aerator. Pressure heads are mostly positive for the entire spillway length for the original design TR-1. Along the flip bucket ($x > 75.6$ m) the pressure values are increased considerably. Only at two locations pressure head depressions caused negative values to be recorded. First depression occurs just at the upstream of the spillway crest. The presence of negative pressure at this location is recorded previously in literature (Vischer and Hager, 1997). However this point is not critical in terms of cavitation. The second depression point lies within the straight part of the spillway approximately at $x = 25$ m with a pressure head value of -4 m. In order to understand the cavitation risk one has to calculate the cavitation number, σ , (Eqn. 1) at those locations. If the cavitation number is less than 0.2, this means that there is a risk of cavitation at that location (Falvey, 1990).

$$\sigma = \frac{p - p_v}{\rho V^2 / 2} \quad (1)$$

Here p and p_v are the pressure and vapor pressure respectively; whereas ρ is the density of water and V is the average velocity.

Variation of the cavitation number along the straight part of the spillway is plotted in Figure 5. Considering the original design, TR-1, starting from $x=25$ m where a pressure depression occurs, the cavitation number drops below 0.2 and stays mostly below that level through the rest of the spillway. In order to prevent the cavitation risk an aerator is designed on the spillway. The piers on the crest of the

spillway is elongated up to the straight part of the spillway ($x=13.3$ m) and between those piers, deflectors with various heights are tested. In design TR-4, deflectors which has a height of 0.4 m and a length of 4.2 m are installed between the piers (Figure 6). The length of the water nappe obtained as a result of these deflectors is approximately 12.5 m. Pressure head values along the spillway for this new design (TR-4) is shown in Figure 4. As seen in this figure, the negative pressure heads occurred in TR-1 are not present in TR-4.

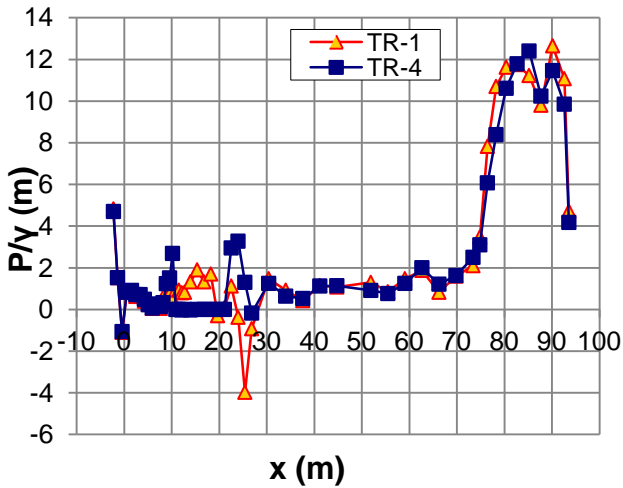


Figure 4: Comparison of the pressure heads over the spillway for the original design (TR-1) and design with aerator (TR-4).

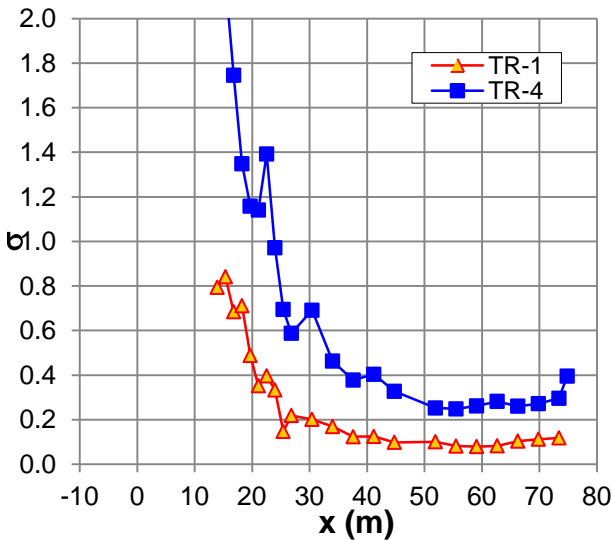


Figure 5: Comparison of the cavitation numbers over the spillway for the original design (TR-1) and design with aerator (TR-4).

Change in the cavitation number for TR-4 is shown in Figure 5 together with TR-1 for the straight part of the spillway. With the aerator utility added to the system, in TR-4 the cavitation number is always larger than 0.2, which

means the risk is eliminated in this design. However, the Froude number at the installation section is low around 3.5 which mean the flow may not be aerated sufficiently and the entrained air may not be preserved up to the lower levels along the spillway where cavitation risk is larger (Falvey, 1990). For that reason the aerator design in TR-4 is modified. The piers on the crest of the spillway is elongated up to $x=26$ m, where Froude number is around 8. At this section aeration rate is larger and the entrained air can be transported until the flip bucket. The dimensions of this aerator are shown in Figure 7, whereas change in the cavitation number along the spillway for this final design is shown in Figure 8.

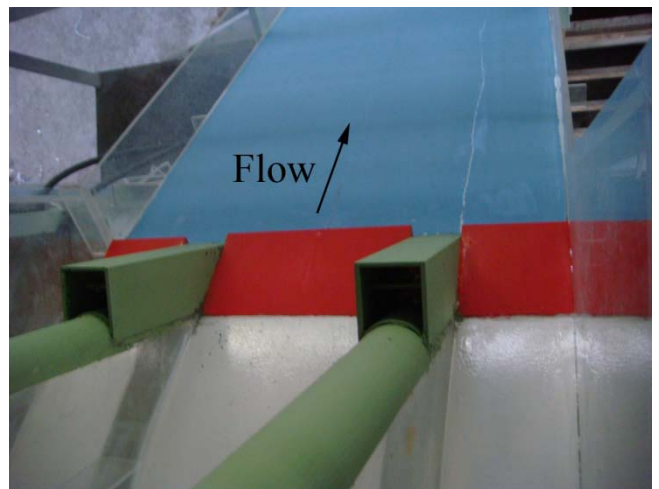


Figure 6: Top view of the aerator system in TR-4.

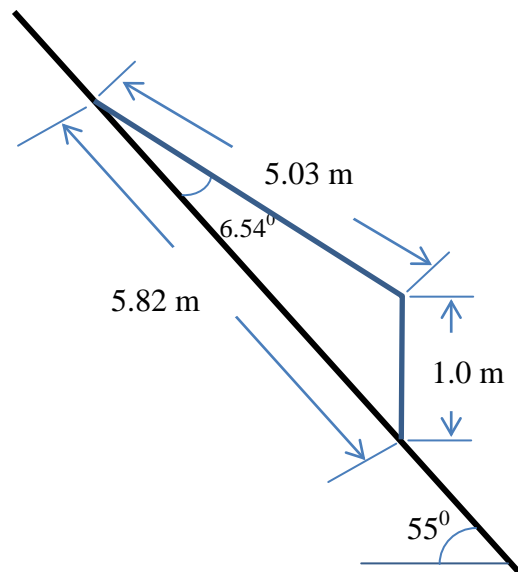


Figure 7: Dimensions of final aerator step.

A numerical simulation of TR-1 is done in the model scale, to see the predictive capabilities of the Flow-3D software. Experimental and numerical results of the pressure head

values and the cavitation number values along the spillway are compared in Figures 9 and 10 respectively. Although the numerical simulation was not able to predict the negative pressure heads occurring over the spillway, it captured the general trend reasonably. More important than that is the behavior of the cavitation number over the spillway. The numerical simulation showed very similar cavitation numbers with the experimental result and it predicted the position where the cavitation risk starts approximately the same with the experimental result.

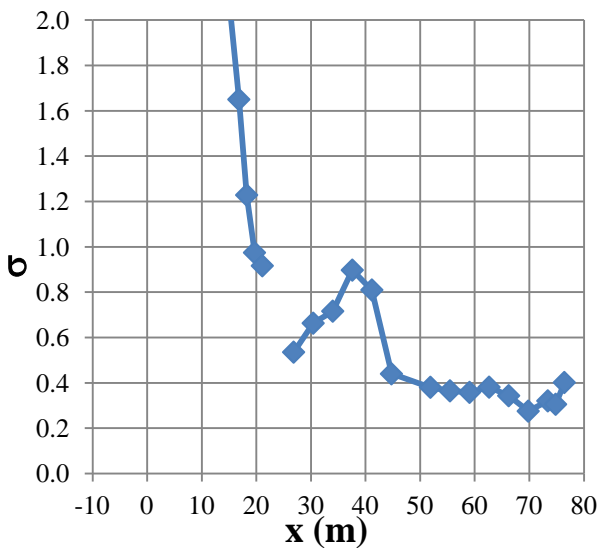


Figure 8: Cavitation numbers over the spillway for the final design.

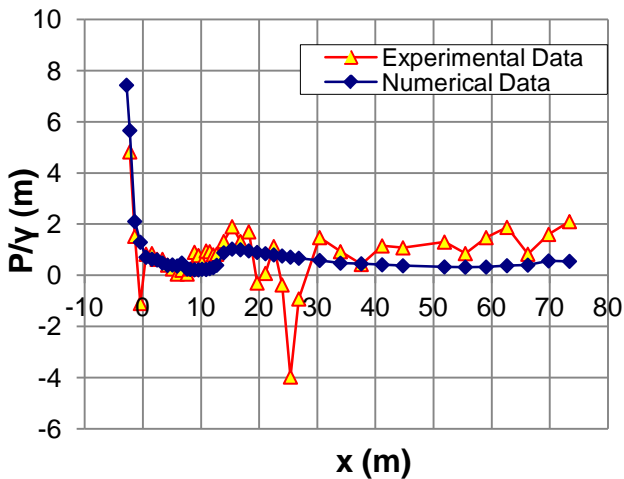


Figure 9: Pressure heads over the spillway obtained from the experiment and the numerical simulation for TR-1.

The differences that occur between the experimental and numerical results are mostly based on the fact that the simulations are steady state solutions which are independent of time whereas in the experiments instantaneous results are recorded which are time dependent. Another reason for this difference may be

related to the different spillway models used in the experiment and simulation. In the experiments, one full and two half openings of the spillway is investigated whereas in the numerical results only a one full opening is modeled. There is no aeration facility in TR-1 which is being simulated. Also the air entrainment rate from the free surface is negligible in the model scale. As a result, the authors do not think that using a numerical model solving only the water phase would introduce significant error.

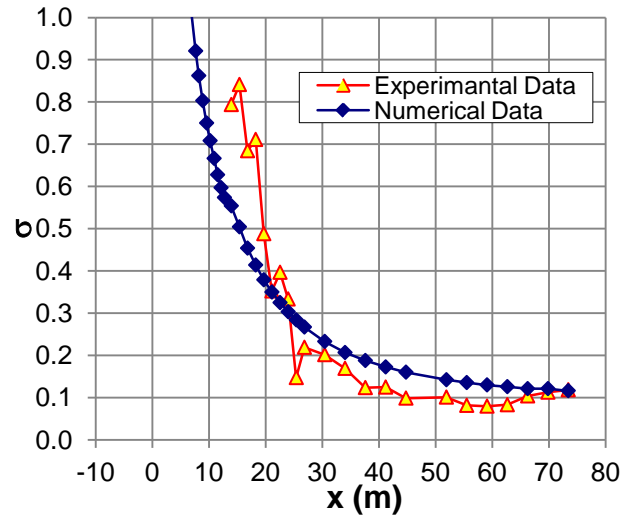


Figure 10: Cavitation number over the spillway obtained from the experiment and the numerical simulation for TR-1.

3D water surface profile obtained from the simulation is shown in Figure 11. There is an increase in the flow depth in the middle of the channel at approximately $x=13$ m. This increase is very local and disappears around $x=21$ m. At around $x=21$ m an increase in the flow depth occurs this time at the two sides of the flow domain (along the pier axes). These two crests get closer to each other and eventually merges at $x=76$ m at the entrance of the flip bucket. This simulated water surface profile is very similar to the one observed during the experiments. In fact there is not a uniform flow depth within any cross-section along the spillway. This means that to characterize a spillway cross-section with a unique cavitation number is not meaningful. Therefore, the lateral change in the cavitation number is plotted for different cross sections in Figure 12. An interesting conclusion can be reached from this plot. At the upstream sections where $x < 51.9$ m, larger cavitation numbers are observed on the sides of the domain (along the pier axes), whereas smallest cavitation numbers are mostly observed along the centerline. Exceptionally at the most upstream two sections ($x=13.9$ m and $x=18.2$ m) the smallest cavitation numbers are observed at approximately 1.5-2 m away from the sides of the domain. However, those values are very close to the ones observed at the centerline

of the domain. In this region, the difference in the cavitation numbers observed at the same cross-section reaches up to 35%. Therefore it is possible to say that the most critical points in terms of cavitation are at the centerline of the spillway for the upstream sections.

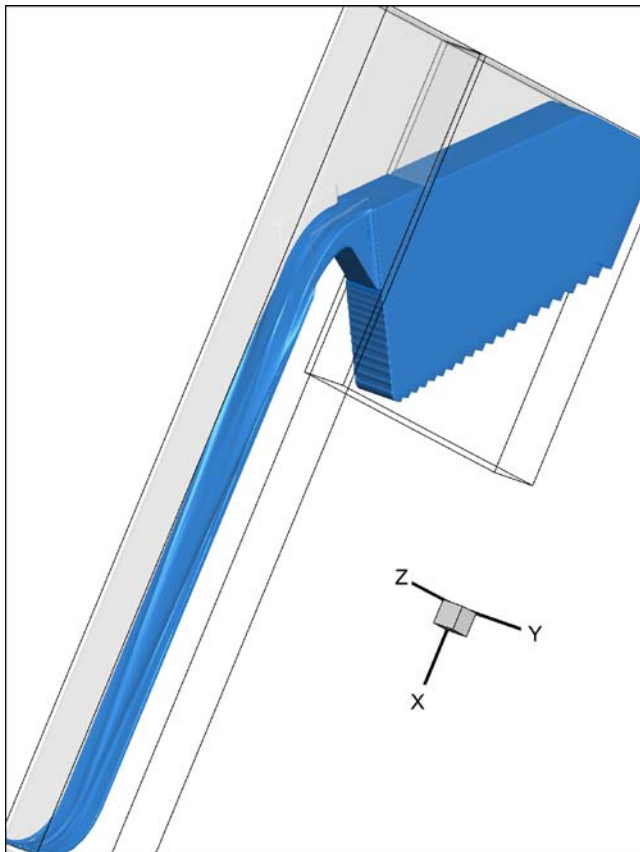


Figure 11: 3D water surface profile obtained from the numerical simulation.

At the downstream part of the domain ($x > 51.9$ m), the smallest cavitation numbers are observed at the sides of the domain whereas the largest values are recorded at the centerline. The difference in the cavitation numbers at the same cross section is around 7.5% in this region. Therefore it is possible to say that the most critical points in terms of cavitation are along the sides of the domain for the downstream sections. According to the simulations starting from $x = 34$ m, the cavitation number drops below the critical threshold of 0.2.

Conclusion

An experimental and numerical study is conducted to evaluate the possible cavitation risk on the spillway of the Laleli dam. Both numerical and experimental results predicted the risk of cavitation approximately at the same location. Using the advantage that with the numerical simulation one can get the cavitation number all over the

spillway surface, an interesting conclusion is reached. Such that at the upstream part of the spillway ($x < 51.9$ m), the midpoints in between the piers are critical in terms of cavitation whereas at the downstream location ($x > 51.9$ m) the points which are aligned with the pier axes are critical. It is also shown experimentally that the risk of cavitation is eliminated with an aerator added to the spillway where the cavitation numbers all over the spillway were larger than 0.2.

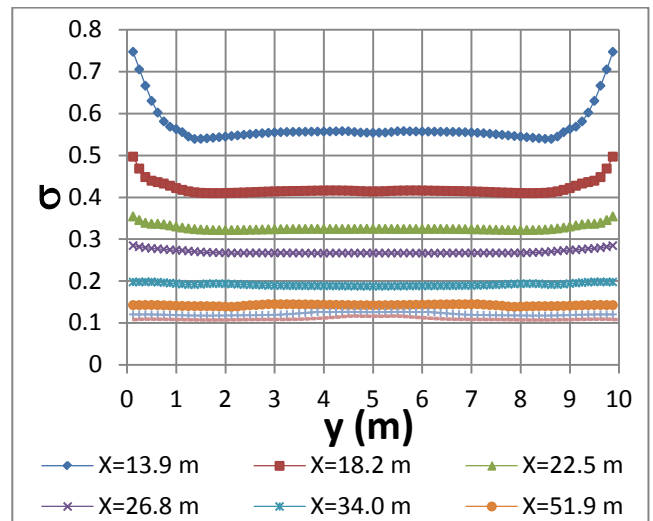


Figure 12: Lateral change in the cavitation number over the spillway for different cross-sections.

References

- Dargahi, B. (2006). *Experimental Study and 3D Numerical Simulations for a Free Overflow Spillway*. Journal of Hydraulic Engineering, 132(9), pp. 899-907.
- Falvey, H. T. (1990). *Cavitation in Chutes and Spillways*. A Water Resources Technical Publication Engineering Monograph no:42: US Bureau of Reclamation.
- Kokpinar, M. A. and Gogus, M. (2002). *High Speed Jet Flows Over Spillway Aerators*. Canadian Journal of Civil Engineering, 29, pp. 888-898.
- Pfister, M. (2011). *Chute Aerators: Steep Deflectors and Cavity Subpressure*. Journal of Hydraulic Engineering, 137(10), pp.1208-1215.
- Unami, K., Kawachi, T., Babar, M. M., and Itagaki, H. (1999). *Two-Dimensional Numerical Model of Spillway Flow*. Journal of Hydraulic Engineering, 125(4), pp. 369-375.
- Vischer, D. L., and Hager, W. H. (1997). *Dam Hydraulics*. Chichester: John Wiley & Sons.